An Algorithm for the Characterization of Digital Images of Pigmented Lesions of Human Skin

Laura Y. Mera-González[a], José A. Delgado-Atencio[a], Juan C. Valdiviezo-Navarro[a] and Margarita Cunill-Rodríguez[a].

[a]Universidad Politécnica de Tulancingo, Ingenierías No. 100, Tulancingo, Hidalgo, México.

ABSTRACT

Melanoma is the most deadly form of skin cancer in human in all over the world with an increase number of victims yearly. One traditional form of diagnosis melanoma is by using the so called ABCDE rule which stands for Asymmetry, Border, Color, Diameter and Evolution of the lesion. For melanoma lesions, the color as a descriptor exhibits heterogeneous values, ranging from light brown to dark brown (sometimes blue reddish or even white). Therefore, investigating on color features from digital melanoma images could provide insights for developing automated algorithms for melanoma discrimination from common nevus. In this research work, an algorithm is proposed and tested to characterize the color in a pigmented lesion. The developed algorithm measures the hue of different sites in the same pigmented area from a digital image using the HSI color space. The algorithm was applied to 40 digital images of unequivocal melanomas and 40 images of common nevus, which were taken from several data bases. Preliminary results indicate that visible color changes of melanoma sites are well accounted by the proposed algorithm. Other factors, such as quality of images and the influence of the shiny areas on the results obtained with the proposed algorithm are discussed.

Keywords: Algorithm, melanoma, common nevus, dermatological, dermatoscopic, HSI, hue.

1. INTRODUCTION

Cutaneous melanoma is nowadays one of the leading cancers around the world[1] and is one of the three types of skin cancer, the most deadly and difficult to diagnose. The incidence of this type of skin cancer has representatively increased representatively in Mexico,[2,3] making necessary to use different techniques for its early detection of it. Melanoma is originated from the cells called melanocytes, which are found in the epidermis-dermis interface human skin.[4] Melanocytes play an important role in humans as they are responsible for the production of a pigment called *melanin* which gives the color to skin, eyes and hair.

There exist different algorithms for the analysis of melanocytic lesions to determine whether a pigmented skin lesion is melanoma or non. Common techniques include Pattern analysis, Menzies, the 7 points checklist and the so-called ABCDE rule of dermoscopy.[5–7] The last one is an usual way of diagnosing melanoma, ABCDE is a rule that specifies a list of visual features associated with malignant melanocytic lesions (Asymmetry, Border structure, Color variation, Diameter and Evolution of the lesion).[8] From the examination of these features is possible to discern common nevus from melanoma, since, this rule yields different results for both of them. As is mentioned in Ref. [8,9], color is an important descriptor that exhibit the variation of tone in a pigmented skin lesion, for example, the colors present in cutaneous melanoma can be white, red, black light brown, dark brown and blue-gray.[6]

The use of skin imaging has become an effective method in the diagnosis of melanoma and other pigmented skin lesions. In Ref. [7] the author describes a technique called TBP (Total Body Photography) in which the patients with pigmented skin lesions are photographed with the purpose of classify and document the lesions for future follow up. Dermoscopy, also known as *epiluminescence microscopy*, is a noninvasive in vivo technique, that uses optical magnification and either liquid immersion and low angle-of-incidence lighting or cross-polarized lighting that minimize surface reflection and enables examination down to the dermo-epidermal junction, i.e., making subsurface structures more easily visible when compared to conventional clinical images.[7,10]

Further author information: (Send correspondence to laura.mera@upt.edu.mx, Tel. +52 775 133 22 89

Applications of Digital Image Processing XXXVII, edited by Andrew G. Tescher, Proc. of SPIE Vol. 9217, 921718
 · doi: 10.1117/12.2062425

There are several alternative methods for the analysis of pigmented skin lesions that allow clear discrimination between melanomas and common nevus. For example, in Ref. [11] the author develops a system to obtain the percentage of the skin lesion containing absolute shades of reddish, bluish, grayish and blackish areas and the number of those color shades present within the skin lesion in dermatoscopy images. In Ref. [12] the author discusses the diagnostic potential of PCA (Principal Component Analysis)) for recognition distant skin melanoma. In Ref. [13] skin lesion color was investigated for discriminating malignant melanoma lesions from benign lesions in clinical images determining color characteristics of melanoma using color histogram analysis over a training set of images. Several color descriptors have been applied to melanoma detection, including variation of hues,[14] red, green and blue (RGB) color channel statistical parameters,[15–17] color variation detection using analytical color techniques,[18] spherical color coordinates and (L, a*, b*) color coordinate features.[19]

In this research, an algorithm to discriminate melanoma from common nevus is presented based on measuring the tone from different sites from dermatological and dermoscopic digital images of melanoma an common nevus. Using the component H of the HSI color space, demonstrating through numerical values of H that in melanoma there is a greater range of variation in hue regarding nevus images. In Section 2 a detailed explanation about the materials and the methodology used for this research is presented. We describe the segmentation technique used and the method to find the hue variation in images of pigmented skin lesions. In Section 3 we present the results and a comparison obtained of hue variations computed from nevus and melanoma images.

2. MATERIALS AND METHODS

2.1 Data acquisition

In order to evaluate the performance of our algorithm, two representative set of digital images of common nevus and melanomas were processed. The data sets were selected from three public databases found on the internet as described below:

- Dataset A: contains 17 dermatological images of melanoma, obtained from the Dermatology Information Service (Dermis) available at Ref. [20]. The site offers an atlas of images made with differential diagnoses, clinical cases and additional information about almost all skin diseases. This service has the cooperation between the Clinical Department of Social Medicine (University of Heidelberg) and the Department of Dermatology (University of Earlangen).
- Dataset B: consists of 52 dermatological images (35 common nevus and 17 melanomas), obtained from the Atlas of Dermatology of the Medical School of the University Hospital Arnau in Vilanova, Spain.[21]
- Dataset C: consists of 11 dermoscopic images (6 melanomas and 5 nevus), acquired from an Atlas of dermoscopy of the Department of Dermatology at Bispebjerg Hospital, Copenhagen NV, Denmark; this presents different cases of skin diseases and their diagnosis by Kaare Weismann M. D., Ph. D., Henrik Lorentzen M. D. and and Mads F. R..[22]

In order to investigate the influence of the image quality in the performance of the algorithm, a phantom tissue was made, whose optical properties and structure were similar to pigmented skin lesions (See Figure 1). The phantom was made of a polyurethane varnish base and catalyst for polyurethane varnish in equal portions, titanium dioxide particles (TiO2) and coffee particles to simulate a lesion.

An optical system was mounted to acquired phantom images, as is shown in Figure 2. The system comprises an illumination stage and a recording system. The illumination channel was comprised by a light source model Fiber Lite® MH-100 (Metal Halide machine vision illuminator, Dolan-Jenner) whose luminous energy was couple to one end of a multi-fiber optical fiber with diameter of 12.5 mm. The other end of the fiber provided a divergent beam that was collimated with a 47.5 mm diameter lens and 10 mm focal length. A neutral density filter (model 946, Newport) was placed in front of the lens, followed by a 35 mm diameter linear polarizer. The images were registered by a CCD multispectral camera (model AD-080GE, JAI) progressive scan, followed by a second linear polarizer. The phantom surface was placed perpendicular at the point of interception between the optical axis of the recording system and the optical axis of the illumination channel. The working distance of the acquisition

Figure 1. Image of a phantom tissue prepared with a polyurethane varnish base and catalyst for polyurethane varnish in equal portions, titanium dioxide particles (TiO2) and coffee particles to simulate a skin lesion.

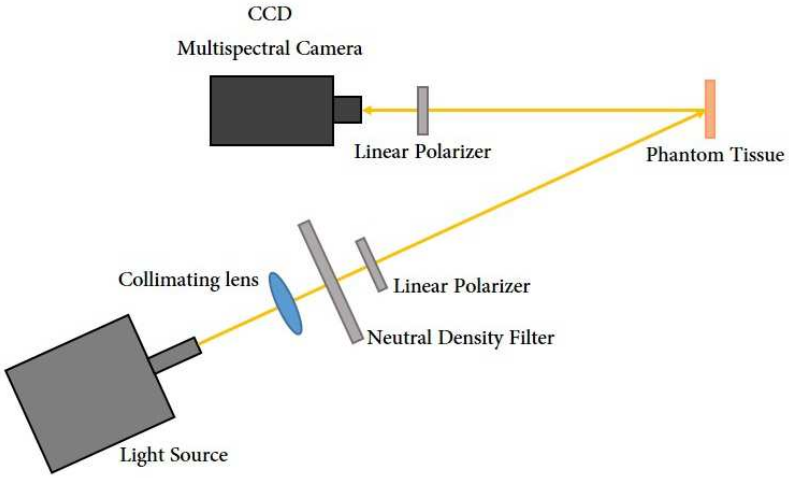

Figure 2. Optical setup used to register phantom images with two different illumination conditions.

system was approximately 24 cm and a field of view 3 cm. The aim of this experiment was to test our algorithm in images under two different illumination conditions.

Once the optical system was mounted, a pair of phantom images were acquired. The first image was captured with a crossed polarizer relative to each other in order to have a image without shine, as illustrated by Figure 3(a). The second image was acquired with the parallel polarizers, having a shiny image in some areas, displayed in Figure 3(b).

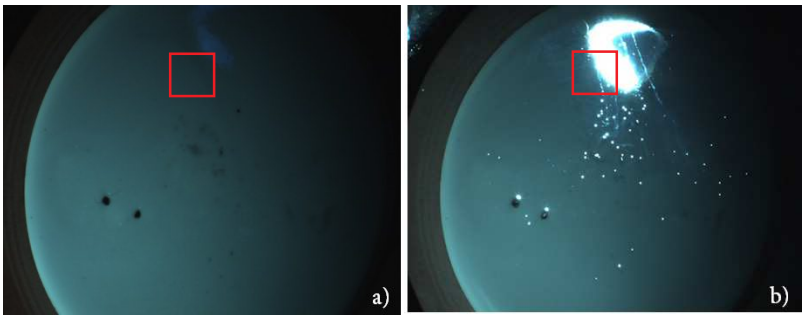

Figure 3. Phantom images. a) Phantom illuminated through crossed polarizers. b)Phantom illuminated through parallel polarizers.

2.2 Data processing

The main objetive of this study is to measure the hue of certain areas of dermatological and dermoscopic digital images of pigmented skin lesions through an algorithm developed in Matlab R2012b® to find the variation of color in common nevus and melanomas.

The proposed algorithm architecture can be seen in Figure 4. A digital image of the lesion is introduced to the algorithm, which segments the lesion automatically. Then, the hue component of the HSI color model is computed. The hue is then divided in different groups to emphasize its variations around the image. Finally, a diagnosis is made by algorithm based these variations. In following lines we describe each one of these stages.

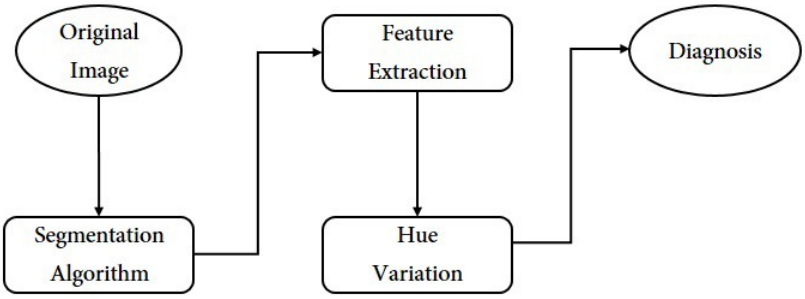

Figure 4. Algorithm architecture.

2.2.1 Image segmentation

The image segmentation step consists on isolating the lesion from the skin. The segmentation process has been realized by thresholding the image in a given value τ. The τ value for this purpose was 0.4. Once the image binary was achieved, as indicated in Figure 5(b), an image complement was obtained as shown by Figure 5(c). Finally, we performed the and operation between the image complement and the respective R, G and B components of the original image to generate a segmented image as can be observed in Figure 5(d).

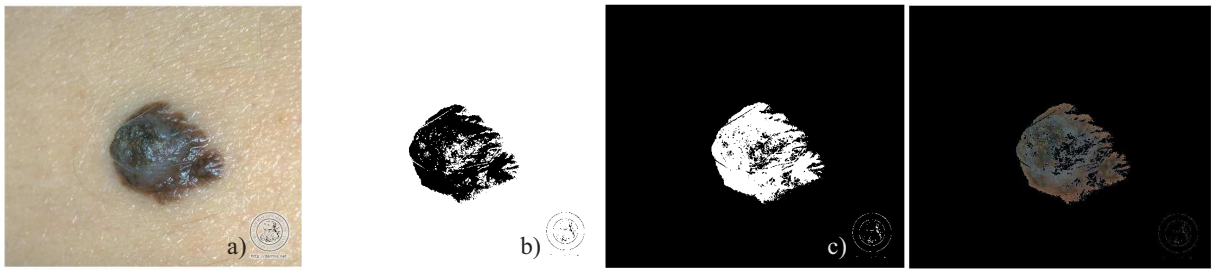

Figure 5. Image segmentation of the pigmented area. a) Original image. b) Binary image. c) Complement image. d) Segmented lesion.

2.2.2 Feature extraction

The feature extraction step is based on the ABCDE rule, which is commonly used by dermatologists to visually diagnose melanoma. The aim of this paper is to characterize pigmented skin lesions based on their color because, for melanoma lesions, the color exhibits heterogeneous values as mentioned in Section 1. Thus, the feature extracted from the segmented images corresponds to the range of variation of the hue.

The measurement of hue in images of common nevus and melanoma was performed based on the HSI (Hue, Saturation and Intensity) color space. Hence, a color space transformation was necessary given that the segmented images are coded in the RGB color space. For this transformation, the following equations are used:[23]

$$H = \cos^{-1}[\frac{\frac{1}{2}[(R-G)+(R-B)]}{\sqrt{(R-G)^2+(R-B)(G-B)}}] \quad (1)$$

$$S = 1 - \frac{3min(R,G,B)}{R+G+B} \quad (2)$$

$$I = \frac{1}{3}(R+G+B) \quad (3)$$

For this research, only the H component is necessary to determine the hue variations from the segmented lesions. According to Eq. (1), hue values are in the range from 0 to 360 degrees, in which, spatially 0°, 120° and 240° correspond to red, green and blue colors, respectively.

2.2.3 Hue variation measurement

Since the segmented image contains black hues with a value of 90° corresponding at background, it results necessary to assign a value of NaN to all pixels in that region. Because the red hues are spatially located at 0° and close values, as well as at 360° and close values, we decided to replace all values between 330° and 360° for 0° with the purpose of avoid confusion in the algorithm, leaving the range of hue variation between 0 and 330 degrees.

In order to identify key changes of hue in common nevus and melanomas, the range of 0° to 330° was divided into 22 groups of 15 degrees each one. One different color was assigned to each group to observe the hue variation in a new RGB image, as illustrated by Figure 6.

Once the new hue component of the segmented image with the corresponding changes was computed, its minimum (H_{min}) and maximum (H_{max}) hue value were found. Finally, to know the hue variation in the segmented lesion, the difference between the maximum and minimum of hue values was calculated, i.e., $Var_{hue} = H_{max} - H_{min}$.

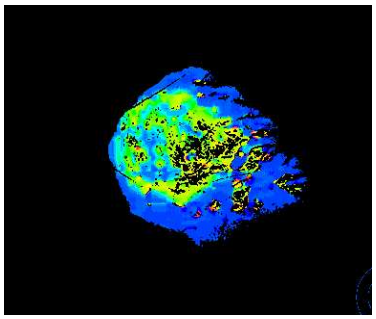

Figure 6. Image of lesion skin, which presents the hue variation through of different color groups.

3. RESULTS AND DISCUSSION

As mentioned before, the main purpose of this research is to realize a discrimination between common nevus and melanomas based on their color variation. In the study presented in this paper, 40 digital images of unequivocal melanomas and 40 images of common nevus, taken from several databases, as mentioned in Section 2.1, were evaluated. The tests were realized on both dermatological and dermoscopic images in order to determine if image quality was an influence in the expected results. Figure 7 presents a comparison between the segmentation process and hue grouping in a melanoma image and a nevus image.

As explained in the previous section, our algorithm is able to extract the H component to obtain the numeric range of color variation in lesions based in the difference between minimum and maximum hue value. Table 1 summarizes some results of hue variation computed from nevus and melanoma images, respectively.

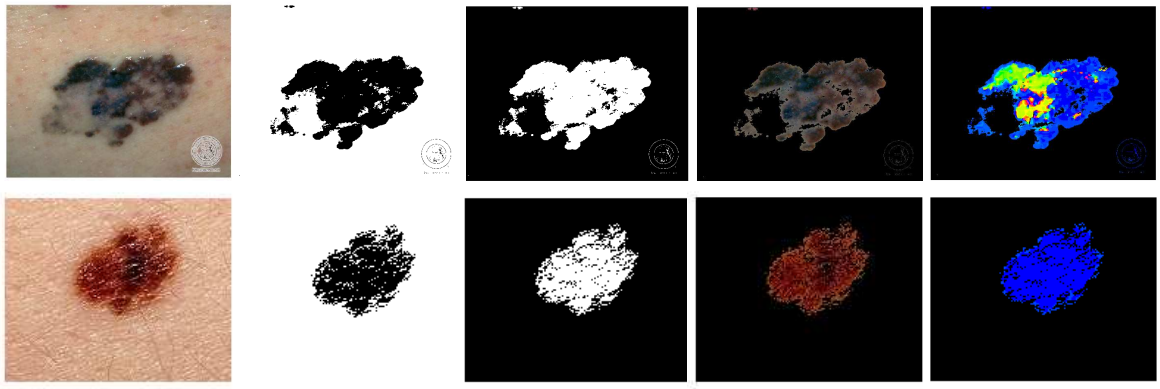

Figure 7. Top row: corresponds to the segmentation process and grouping colors in melanoma image. Bottom row: presents the results of segmentation process and grouping colors in a nevus image.

IMAGE	HUE MINIMUM VALUE (H_{min})	HUE MAXIMUM VALUE (H_{max})	HUE VARIATION Var_{hue}
Dermatological melanoma	0.00013938°	330°	329.9999°
Dermatological melanoma	0.00019275°	330°	329.9999°
Dermatological nevus	0.0001285°	23.2560°	23.2558°
Dermatological nevus	0.00047680°	51.0517°	51.0512°
Dermoscopic melanoma	0.0001766°	330°	329.9999°
Dermoscopic melanoma	0.0002157°	330°	329.9998°
Dermoscopic nevus	0.00012242°	7.8154°	7.8153°
Dermoscopic nevus	0.0001874°	21.3939°	21.3937°

Table 1. Comparison of hue variation of some melanomas and nevus.

3.1 Dermatological images

The algorithm was applied to 35 dermatological digital images of common nevus and 34 melanomas, examples can be seen in Figure 8. According to our results, for pigmented lesions of melanoma $H_{min} = 0.00013938°$ and $H_{max} = 330°$, therefore, in dermatological digital images of melanoma $Var_{hue} = 329.9999°$. While in nevus, $Var_{hue} = 51.0516°$ because, $H_{min} = 0.0001285°$ and $H_{min} = 51.0517°$.

3.2 Dermoscopic images

Similarly, the algorithm was tested on dermoscopic nevus and melanoma digital images to measure the hue variation in the pigmented region, see Figure 9. In these cases our algorithm found that for melanoma lesions $H_{min} = 0.0001766°$ and $H_{max} = 330°$, then, $Var_{hue} = 329.9999°$. For nevus lesions $H_{min} = 0.00012242°$ and $H_{max} = 21.3939°$, then, $Var_{hue} = 21.3938°$.

3.3 Determination of influence of shiny areas

Finally, in order to determine the influence of shine in images, we applied our algorithm on a same area of the phantom image, marked region with red box, as indicated in Figure 3, presented in Section 2.

The hue value for the marked region of Figure 3(a) was equal to 192.91°, while the hue value for the marked region of Figure 3(b) was equal to 166.81°. Therefore, the results indicated that indeed the shine is a parameter of image quality which significantly influences in the hue value.

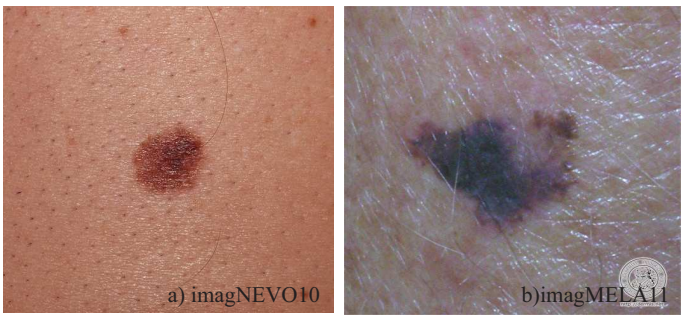

Figure 8. Examples of dermatological digital images. a) Common nevo image. b) Melanoma image.

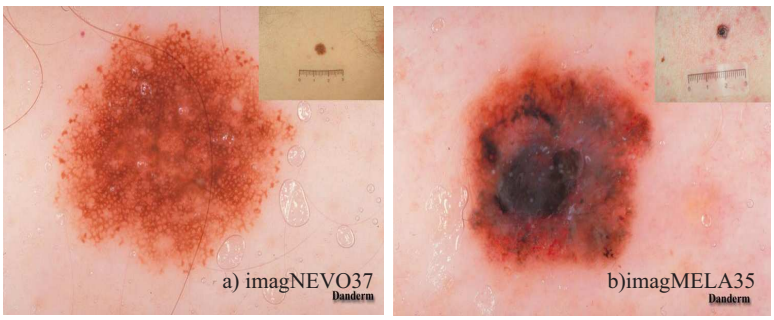

Figure 9. Examples of dermoscopic digital images. a) Melanocytic nevo image. b) Melanoma image.

Two factors we could consider for processing images. First,the presence of hair on the images is primarily a influential factor in the segmentation of the lesion, and subsequently, for obtaining the hue variation, because sometimes it could have a higher value than in the area in which is located the lesion. This case was present only in 2.5% of our processed images. Second, to avoid problems of segmentation is important to have images with the fewest possible of skin areas, so for the algorithm will be easier to extract the section of interest.

The 17.5% of our melanoma images present homogeneous colors, therefore, when they were processed with the algorithm, a range of hue variation less than 50° was obtained.

4. CONCLUSIONS

An automatic algorithm for color measurement in dermatological and dermoscopic images of common nevus and melanoma lesions, as well as in tissue phantoms was developed. The result of applying this algorithm reflected the evident hue variation in the processed images. The general range of hue variation in dermatological and dermoscopic melanoma lesions was between 0.0013938° and 330°, while for dermatological and dermoscopic images nevus it was between 0.00012242° and 51.00517°. The grouping colors in a pigmented skin lesions allows to observe the evident hue variation in melanoma lesions and the homogenous hue in common nevus.

Finally, the proposed algorithm was tested in a pair phantom images with the purpose of check that shine in an image influences on the numerical hue value, shine that is often found in dermatological images.

ACKNOWLEDGMENTS

Laura Y. Mera-González is thankful with the National Council of Science and Technology (CONACyT) for a scholarship. José A. Delgado-Atencio thanks to SEP-PROMEP for partial financial support throug a project.

REFERENCES

[1] Green, A., Martin, N., McKenzie, G., Pfitzner, J., Quintarelli, F., Thomas, B. W., O'Rourke M., and Knight N., "Computer image analysis of pigmented skin lesions," Melanona Res., Papers 1(4), 231-236 (1991).

[2] Ruíz, A., Escoabar, G., de la Barrera, F., Herrera, A., Padilla, A., Suchil, and L., G., "Epidemiología del melanoma de piel en México.," Rev. Inst. Nac. Cancerol., Papers 44(4), 168-174 (1998).

[3] González, N. E. and Flores, A. Y., "El melanoma en México," Revista de Especialidades Médico-Quirúrgicas., Papers 15(3), 161-164 (2010).

[4] Fukunaga, M., Martínez, G., Liu, Z-J., Kalabis, J., Mrass, P., Weninger, W. , Firth, S. M., Planque, N., Perbal, B., and Herlyn M., "CCN3 controls 3D spatial localization of melanocytes in the human skin through DDR1," JCB, Papers 175(4), 563-569 (2006).

[5] Argenziano, G., Fabbrocini, G., Carli, P., De Giorgi, V., Sammarco E., and Delfino, M., "Epiluminescence microscopy for the diagnosis of doubtful melanocytic skin lesions, comparison of the abcd rule of dermatoscopy and a new 7-point checklist based on pattern analysis," Arch. Dermatol., Papers 134(12), 15631570 (1998).

[6] Capdehourat, G., Corez, A., Bazzano, A., Alonso, R., and Musé, P., "Toward a combined tool to assist dermatologists in melanoma detection from dermoscopic images of pigmented skin lesions," Pattern Recognition Letters, Papers 32(16), 21872196 (2011).

[7] Wang, S. Q. and Hashemi, P., "Noninvasive Imaging Technologies in the Diagnosis of Melanoma," Semin Cutan Med Surg., Papers 29(3), 174-184 (2010).

[8] Friedman, R. J. and Rigel, D. S., "The clinical features of malignant melanoma," Dermatol Clin., Papers 3(2), 271-283 (1985).

[9] Nachbar, F., Stolz, W., Merkle, T., Cognetta, A. B., Vogt, T., Landthaler, M., Bilek, P., Braun-Falco, O., and Plewig, G., "The ABCD rule of dermatoscopy: High prospective value in the diagnosis of doubtful melanocytic skin lesions original," J Am Acad Dermatol., Papers 30(4), 551-559 (1994).

[10] Argenziano, G., Soyer, H. P., and De Giorgi, V., Dermoscopy: A tutorial. Milan, Italy: EDRA Medical Publishing & New Media; (2002).

[11] Ganster, H., Pinz, A., Rohrer, R., Wildling, E., Binder, M., and Kittler, H., "Automated Melanoma Recognition," IEEE Transactions on Medical Imaging, Papers 20(3), 233-239 (2001).

[12] Jakovels, D., Lihacova, I., Kuzmina, I., and Spigulis, J., "Application of principal component analysis to multispectral imaging data for evaluation of pigmented skin lesions," Proc. SPIE 9032, 903204 (2013).

[13] Stanley, R. J., Stoecker, W. V., and Moss, R. H., "A relative color approach to color discrimination for malignant melanoma detection in dermoscopy images," Skin Res Technol., Papers 13(1), 62-72 (2007).

[14] Landau M., Matz H., Tur E., Dvir M., and Brenner S., "Computerized system to enhance the clinical diagnosis of pigmented cutaneous malignancies," Int J Dermatol., Papers 38(6), 443-446 (1999).

[15] Green A., Martin N., Pfitzner J., O'Rourke M., and Knight N., "Computer image analysis in the diagnosis of melanoma," J Am Acad Dermatol., Papers 31(6), 958-964 (1994).

[16] Seidenari S., Burroni M., Dell'Eva G., Pepe P., and Belletti B., "Computerized evaluation of pigmented skin lesion images recorded by a videomicroscope: comparison between polarizing mode observation and oil/slide mode observation," Skin Res Technol., Papers 1(4), 187-191 (1995).

[17] Aitken J. F., Pfitzner J., Battistutta D., O'Rourke P. K., Green A. C., and Martin N. G., "Reliability of computer image analysis of pigmented skin lesions of Australian adolescents," Cancer, Papers 78, 252-257 (1996).

[18] Umbaugh S. E., Moss R. H., and Stoecker W.V., "Automatic color segmentation of images with application to detection of variegated coloring in skin tumors," IEEE Eng Med Biol., Papers 8(4), 43-52 (1989).

[19] Ercal F., Chawla A., Stoecker W. V., Lee H. C., and Moss R. H., "Neural network diagnosis of malignant melanoma from color images," IEEE Trans Biomed Eng., Papers 41(9), 837-845 (1994).

[20] Dermatology Information Service is aviable at dermis.multimedica.de/dermisroot/es/17570/diagnose.htm

[21] Atlas of dermatology is aviable at http://web.udl.es/usuaris/dermatol/Atlasweb/n.html

[22] Atlas of dermatoscopy is aviable at http://www.danderm.dk/derma/section1/index1.html

[23] González, R. C. and Woods, R. E., [Digital Image Processing], 3er edn. Pearson Prentice-Hall, 289-302 (2002).